Supplementary Table Janssen et al.

Table Data collection and refinement statistics

	Sema4D-PlxnB1	Sema6A-PlxnA2	Sema6A	PlxnA2
Data collection				
Space group	*F*222	$C222_1$	$P3_1$	*C*2
Cell dimensions				
a, *b*, *c* (Å)	83.1, 173.4, 482.1	155.5, 159.6, 139.3	97.0, 97.0, 153.1	158.0, 93.1, 62.9
α, β, γ (°)	90, 90, 90	90, 90, 90	90, 90, 120	90, 102.9, 90
Resolution (Å)	50-3.0 (3.10-3.00)*	55-2.2 (2.32-2.20)*	37-2.3 (2.42-2.30)*	50-2.3 (2.42-2.30)*
R_{merge} (%)	11.9 (88.1)	9.9 (66.2)	6.8 (59.8)	12.2 (67.7)
$I/\sigma I$	14.2 (4.5)	7.8 (1.9)	11.1 (1.9)	6.6 (1.6)
Completeness (%)	99.6 (99.3)	94.4 (96.4)	99.6 (99.4)	97.9 (98.8)
Redundancy	4.8 (4.5)	3.8 (3.6)	3.1 (2.9)	2.8 (2.8)
Refinement				
Resolution (Å)	50-3.0	40-2.2	33-2.3	45-2.3
No. reflections	35192	82680	71390	38559
R_{work}/ R_{free} (%)	20.3 / 24.5	19.0 / 23.0	18.5 / 21.9	20.3 / 25.4
No. atoms	8744	9608	9002	5417
Protein	8744	9189	8651	5208
Ligand/ion	0	30	73	27
Water	0	389	278	182
B-factors (Å^2)				
Protein	76.5	50.9	57.8	41.3
Ligand/ion		64.5	66.2	56.3
Water		41.1	41.7	34.0
R.m.s deviations				
Bond lengths (Å)	0.008	0.005	0.009	0.003
Bond angles (°)	1.33	0.92	1.18	0.79

*Highest resolution shell is shown in parenthesis.

Supplementary Figure 1 Janssen et al.

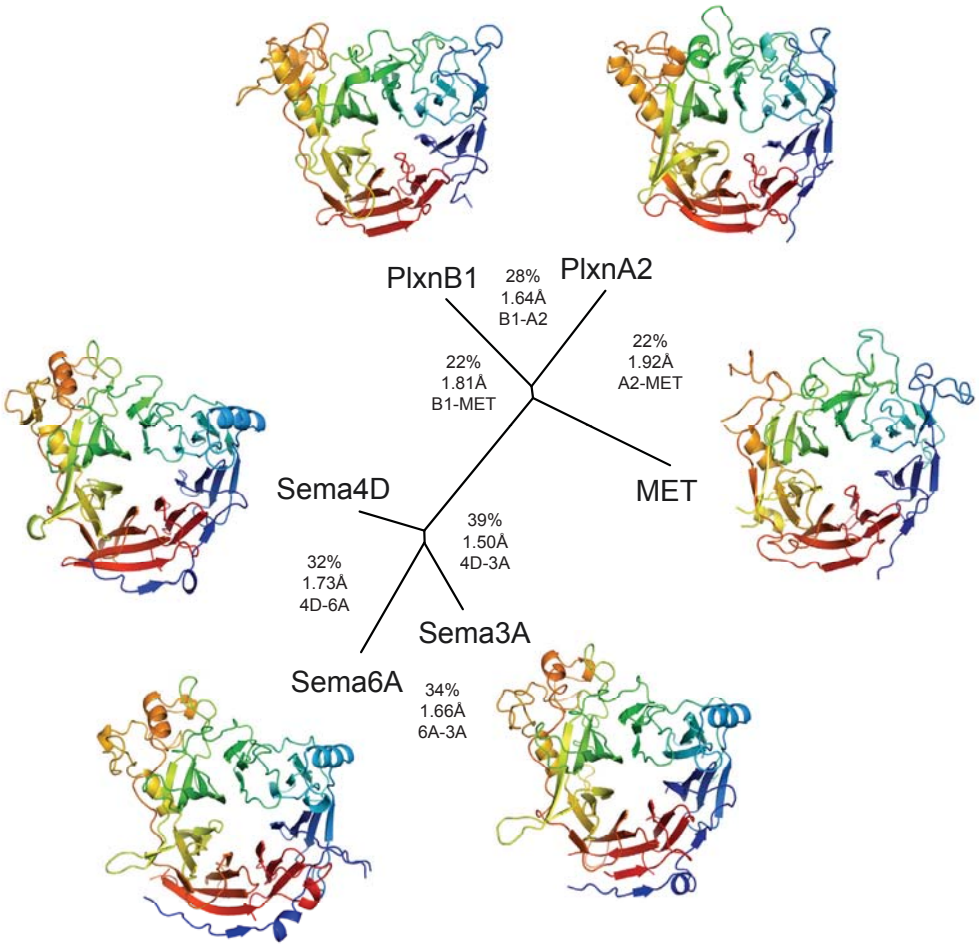

Supplementary figure 1. Structure-based phylogenetic analysis of the sema domain.
a, All available structures of sema domains (Sema4D[5] pdb code 1OLZ, Sema3A[6] pdb code 1Q47, Met receptor[19] pdb code 1SHY and Sema6A, PlxnB1 and PlxnA2 described here) were superposed, a pairwise distance matrix was constructed based on structural similarity with the program SHP[46] and converted into a tree representation with the PHYLIP package (http://evolution.genetics.washington.edu/phylip.html). Structure based sequence identity (%) calculated with the program Indonesia (http://xray.bmc.uu.se/dennis) and Cα atoms rmsds (Å) calculated with SHP are shown for indicated sema domain comparisons. Ribbon representations are "rainbow" colour ramped from blue (N-terminus) to red (C-terminus). The Met receptor sema domain is most homologous to that of plexins.

Supplementary Figure 2 Janssen et al.

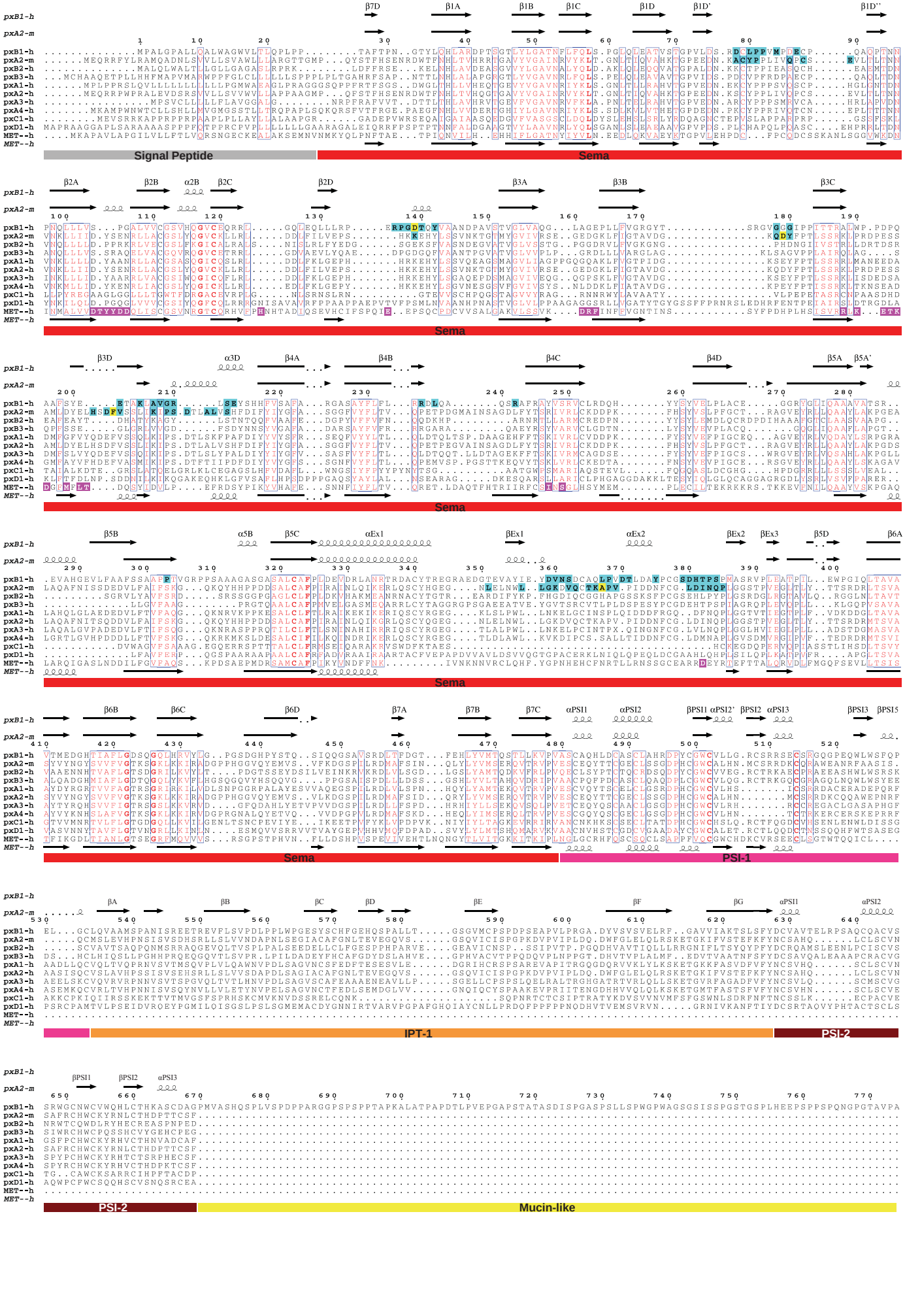

Supplementary Figure 2 Janssen et al.

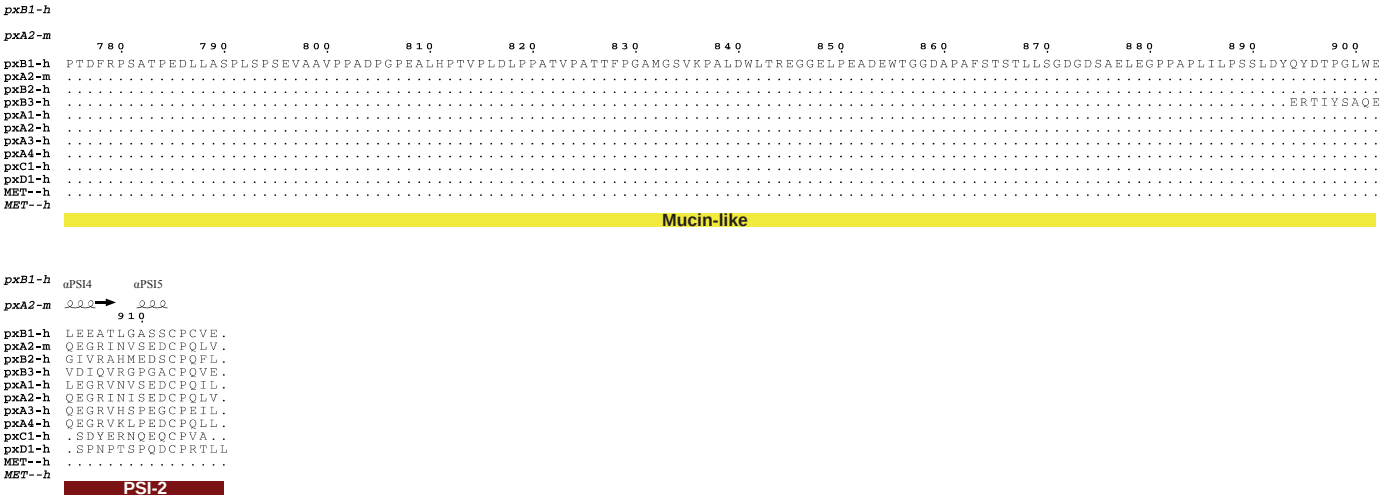

Supplementary figure 2. Sequence alignment of plexin family members and Met receptor.
Sequences of the sema, PSI-1, IPT-1 and PSI-2 domains of all human plexin family members, mouse PlxnA2 and human Met were aligned based on the structures of the sema domains of human PlxnB1, mouse PlxnA2 and human Met[19] (pdb code 1SHY) with Indonesia (http://xray.bmc.uu.se/dennis) and on sequence similarity with ClustalW[48]. Numbering corresponds to the full length human PlxnB1 (including the secretion signal sequence). Secondary structure assignments derived from the crystal structures of $PlxnB1_{1-2}$ and $PlxnA2_{1-4}$ are displayed above the alignment and those from the crystal structure of Met below. Domains are indicated by coloured rectangles below the alignment. Residues in the semaphorin-plexin interface are coloured cyan, residues that were mutated in this study are coloured yellow. Residues in the scatter factor β-chain - Met receptor interaction site[19] are coloured pink and show that the semaphorin interaction site on plexin does not overlap with that of the scatter factor on Met. PlxnB1 contains a 230 residue large insertion within PSI-2 that is predicted to be heavily O-glycosylated and similar in sequence to mucin domains. The figure was prepared with ESPript (espript.ibcp.fr/ESPript/ESPript/).

Supplementary Figure 3 Janssen et al.

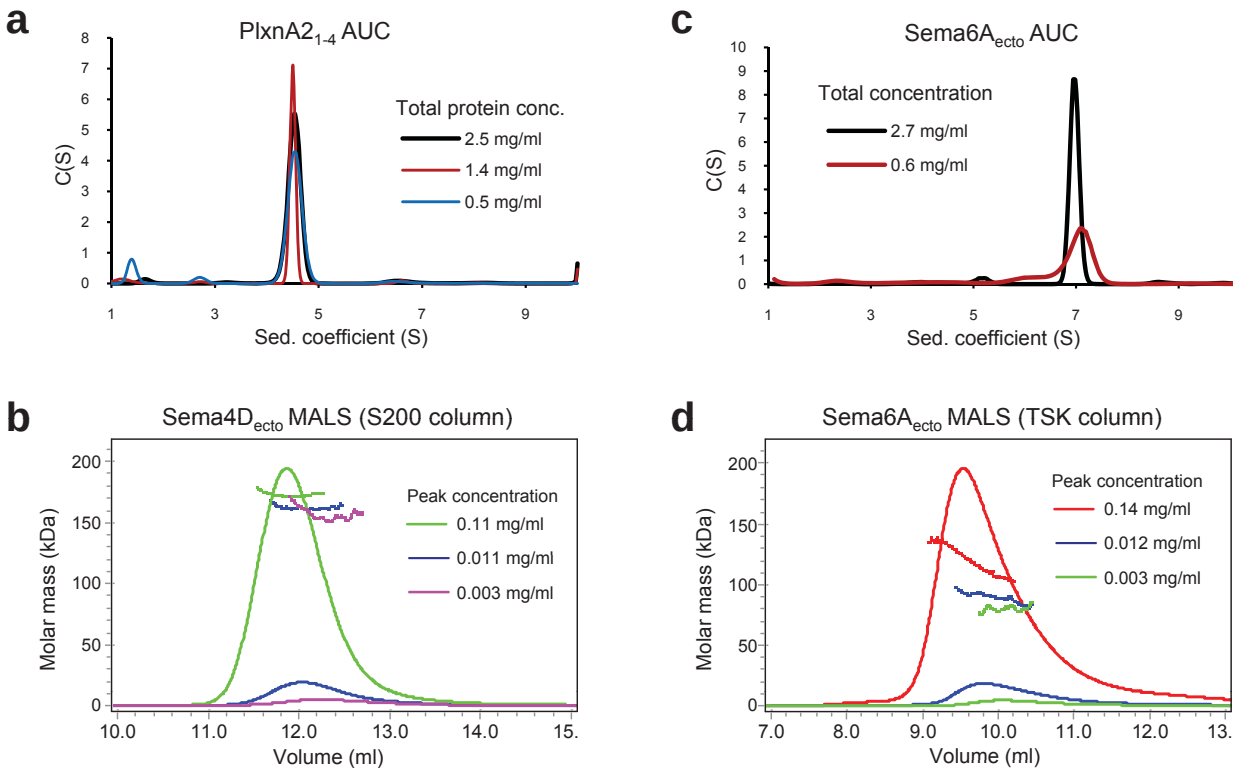

Supplementary figure 3. PlxnA2$_{1-4}$ is a monomer and Sema4D$_{ecto}$ and Sema6A$_{ecto}$ are concentration dependent dimers.

Multi-angle light scattering (MALS) and sedimentation velocity analytical ultracentrifugation (AUC) revealed that PlxnA2$_{1-4}$ is monomeric in solution and that both Sema4D$_{ecto}$ and Sema6A$_{ecto}$ are concentration dependent dimers. The calculated molar mass is 85 kDa for monomeric PlxnA2$_{1-4}$ assuming 12% w/w glycosylation, 180 kDa for dimeric Sema4D$_{ecto}$ assuming 18% w/w glycosylation and 145 kDa for dimeric Sema6A$_{ecto}$ assuming 10% w/w glycosylation. **a**, Sedimentation coefficient distribution of PlxnA2$_{1-4}$ determined by AUC. The main peak at each concentration corresponds to a monomer with a molar mass of 85.7 ± 1.2 kDa, thus PlxnA2$_{1-4}$ is a monomer even at a concentration of 2.5 mg/ml (29 µM). **b**, MALS analysis of Sema4D$_{ecto}$ showing the molar mass (axis on the left) together with the elution profile (axis not shown) at three different concentrations. The weight average molar mass of Sema4D$_{ecto}$ determined at a peak concentration of 0.11 mg/ml is 174 ± 2 kDa and indicates that Sema4D$_{ecto}$ is a dimer. At lower concentrations the elution peaks shift to a larger retention volume and the weight average molar masses are slightly reduced demonstrating that the dimer-monomer balance has shifted somewhat towards the monomer. **c**, Sedimentation coefficient distribution of Sema6A$_{ecto}$ determined by AUC. The main peak at each concentration corresponds to a dimer with a molar mass of 152 ± 6 kDa. **d**, Same as in **b** but for Sema6A$_{ecto}$ and on a different type of column (therefore retention volumes cannot be compared). Sema6A$_{ecto}$ elutes as a monomer-dimer mixture at a peak concentration of 0.14 mg/ml. At lower concentrations the elution peaks shift and the weight average molar masses are reduced indicating that the balance has further shifted towards the monomer. Interestingly Sema6A$_{ecto}$ elutes almost entirely as a monomer at a peak concentration of 0.003 mg/ml indicating that the semaphorin-semaphorin interaction is stronger in Sema4D$_{ecto}$ than in Sema6A$_{ecto}$.

Supplementary Figure 4 Janssen et al.

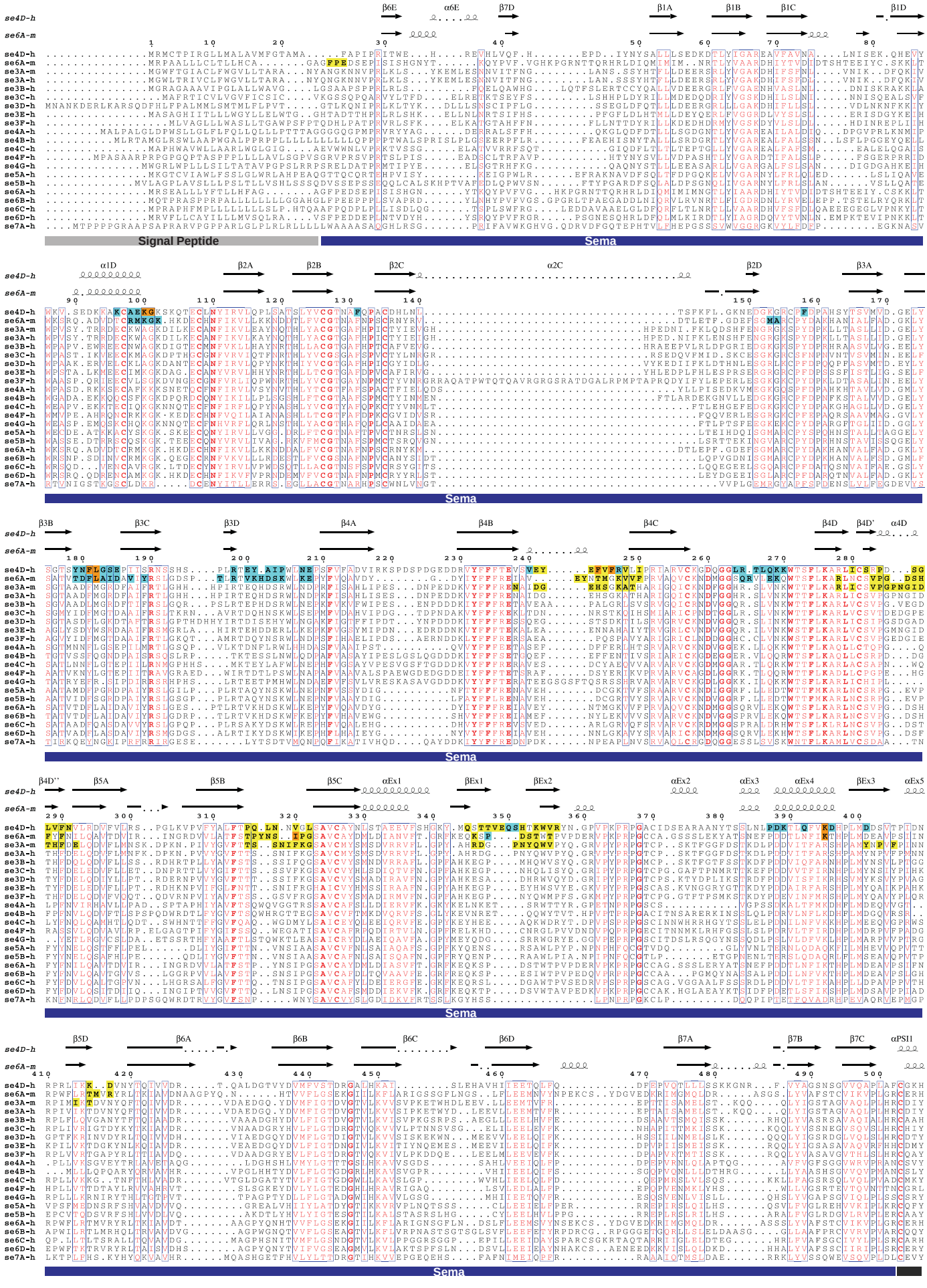

Supplementary Figure 4 Janssen et al.

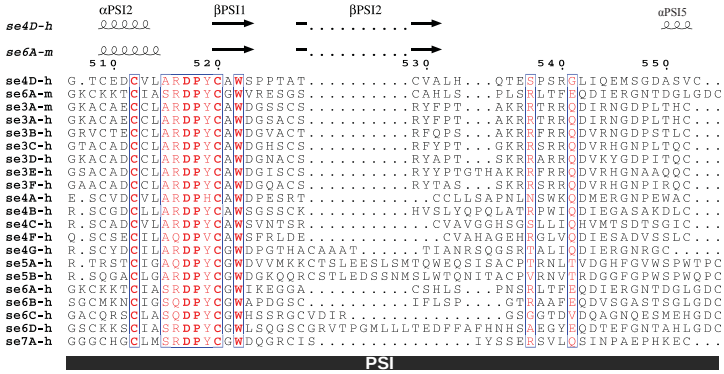

Supplementary figure 4. Sequence alignment of semaphorin family members.
Sequences of the sema and PSI domains of all human semaphorin family members and mouse Sema6A were aligned based on the structures of the sema domains of human Sema4D, mouse Sema6A and human Sema3A[6] (pdb code 1Q47) with Indonesia (http://xray.bmc.uu.se/dennis) and on sequence similarity with ClustalW[48]. Numbering corresponds to the full length human Sema4D (including the secretion signal sequence). Secondary structure assignments derived from the crystal structures of $Sema4D_{ecto}$ and $Sema6A_{ecto}$ are displayed above the alignment. Domains are indicated by coloured rectangles below the alignment. Residues in the semaphorin-plexin interface are coloured cyan, residues that were mutated in this study are coloured orange. Residues in the semaphorin-semaphorin homodimer interface are coloured yellow. The figure was prepared with ESPript (espript.ibcp.fr/ESPript/ESPript/).

Supplementary Figure 5 Janssen et al.

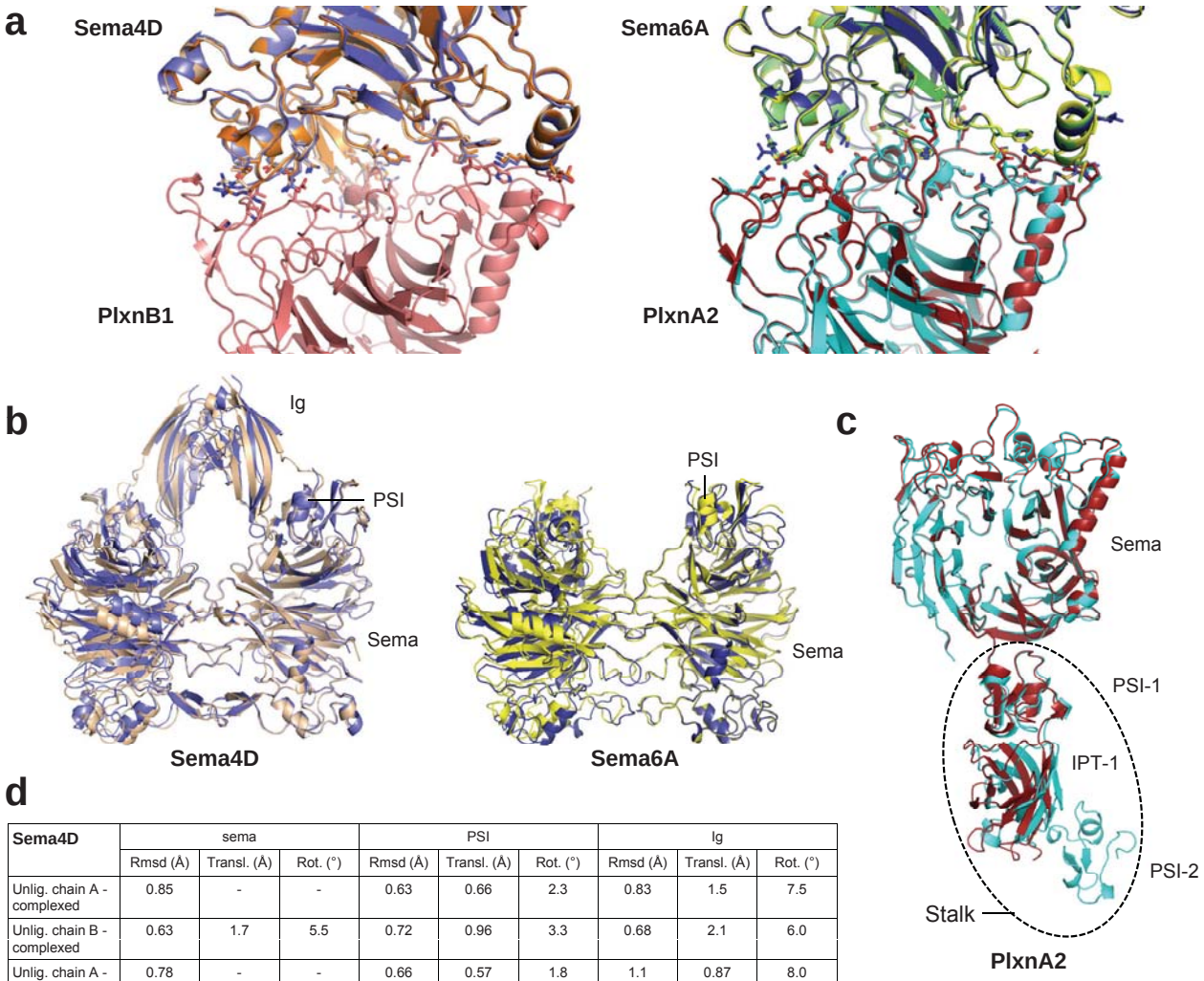

d

Sema4D	sema			PSI			Ig		
	Rmsd (Å)	Transl. (Å)	Rot. (°)	Rmsd (Å)	Transl. (Å)	Rot. (°)	Rmsd (Å)	Transl. (Å)	Rot. (°)
Unlig. chain A - complexed	0.85	-	-	0.63	0.66	2.3	0.83	1.5	7.5
Unlig. chain B - complexed	0.63	1.7	5.5	0.72	0.96	3.3	0.68	2.1	6.0
Unlig. chain A - Unlig. chain B	0.78	-	-	0.66	0.57	1.8	1.1	0.87	8.0

Sema6A	sema			PSI		
	Rmsd (Å)	Transl. (Å)	Rot. (°)	Rmsd (Å)	Transl. (Å)	Rot. (°)
Unlig. chain A - complexed	0.54	-	-	0.84	0.62	10
Unlig. chain B - complexed	0.71	2.5	9.1	0.78	0.43	12.4
Unlig. chain A - Unlig. chain B	0.59	-	-	0.51	0.24	4.3

PlxnA2	sema	PSI-1			IPT-1		
	Rmsd (Å)	Rmsd (Å)	Transl. (Å)	Rot. (°)	Rmsd (Å)	Transl. (Å)	Rot. (°)
Unliganded -complexed	0.59	0.27	1.7	8.3	0.31	6.0	10.8

Supplementary figure 5. There are no large conformational changes upon complex formation.
a, There are no large conformational changes in the semaphorin-plexin interface. Ribbon representation of sema domain based superpositions and stick representation of residues contributing to the semaphorin-plexin interface are shown. Unliganded $Sema4D_{ecto}$[5] (chain A, wheat and chain B, orange) superposed onto complexed $Sema4D_{ecto}$ (slate) (left panel). Superpositions of unliganded $Sema6A_{ecto}$ (chain A, yellow and chain B, lime) onto complexed $Sema6A_{ecto}$ (blue) and unliganded $PlxnA2_{1-4}$ (cyan) onto complexed $PlxnA2_{1-4}$ (dark red) (right panel). **b**, There are no large conformational changes in the semaphorin homodimer upon complex formation. Superpositions, based on one sema domain of a semaphorin dimer, of unliganded $Sema4D_{ecto}$ (wheat) onto complexed $Sema4D_{ecto}$ (slate) (left panel) and unliganded $Sema6A_{ecto}$ (yellow) onto complexed $Sema6A_{ecto}$ (blue) (right panel). **c**, There are no large conformational changes in $PlxnA2_{1-4}$ upon complex formation although the stalk may be inherently flexible. Complexed $PlxnA2_{1-4}$ (red) superposed onto unliganded $PlxnA2_{1-4}$ (cyan), PSI-2 has been omitted from complexed $PlxnA2_{1-4}$ due to disorder in the crystal (see Methods). **d**, Proteins were superposed on the basis of the sema domain. Using these superpositions domain translation, rotation and rmsd's (root mean square deviation, of Cα atoms) were calculated with SUPERPOSE in the CCP4 package[38] to compare the unliganded forms with the complexed ones.

Supplementary Figure 6 Janssen et al.

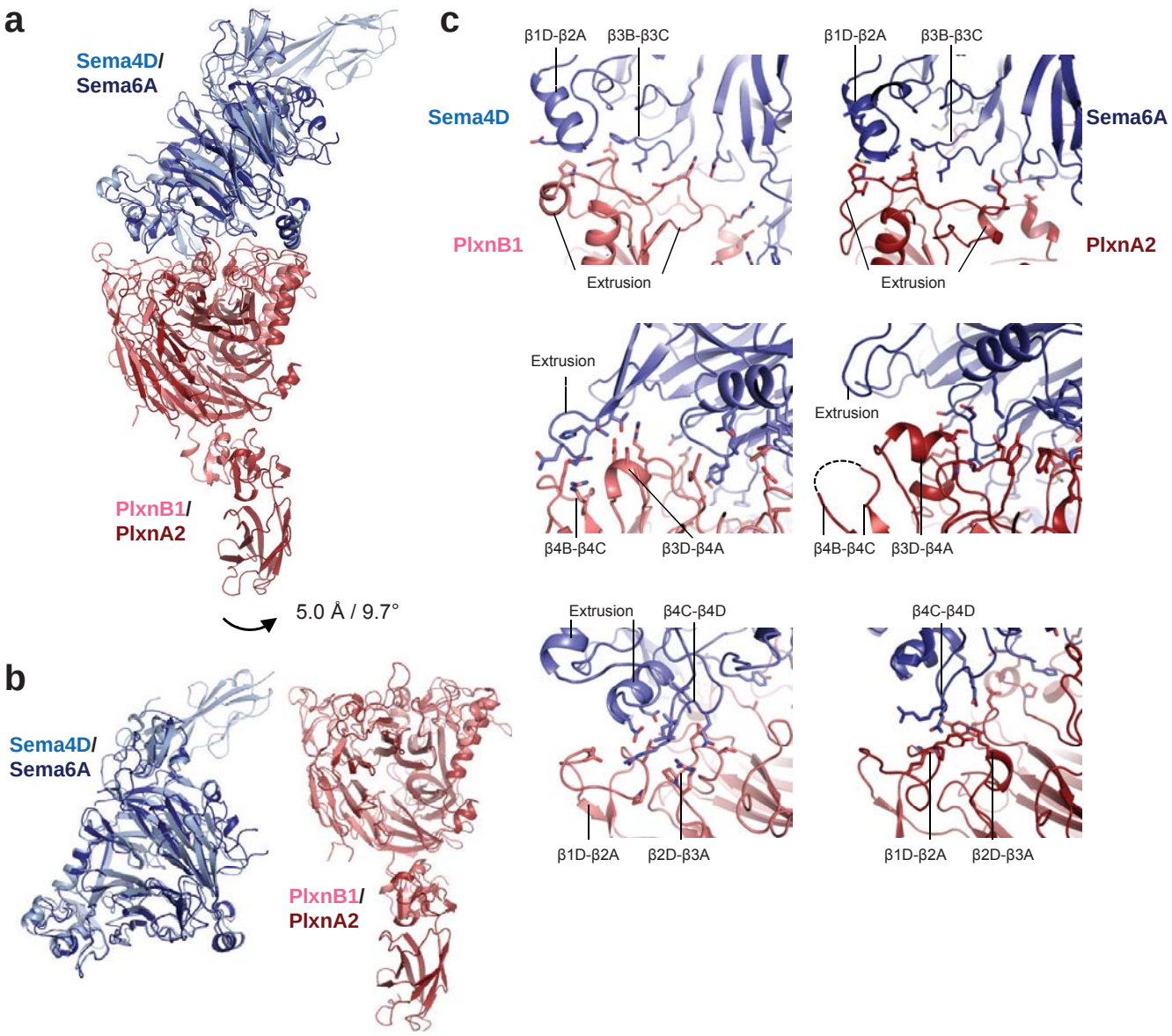

Supplementary figure 6. PlxnB1 and PlxnA2, and Sema4D and Sema6A are very similar, differences in the interface determine specificity.

a, Ribbon representation of superposed PlxnB1$_{1\text{-}2}$-Sema4D$_{ecto}$ and PlxnA2$_{1\text{-}4}$-Sema6A$_{ecto}$ complexes based on the semaphorin sema domain. A difference between the two complexes is reflected in a slightly different position of the plexins, nevertheless overall the complexes are very similar. **b**, Superpositions of Sema4D$_{ecto}$ and Sema6A$_{ecto}$, and of PlxnB1$_{1\text{-}2}$ and PlxnA2$_{1\text{-}4}$ based on the sema domain. **c**, Close-up view of the interface from equivalent positions of the two complexes are shown (left panels PlxnB1$_{1\text{-}2}$-Sema4D$_{ecto}$, right panels PlxnA2$_{1\text{-}4}$-Sema6A$_{ecto}$) with residues contributing to the interface in stick representation (see supplementary fig. 2 and 4 for naming of secondary structure). Overall the semaphorin-plexin interface is similar between the two complexes, nevertheless there are significant differences that may reflect class specificity.

Supplementary Figure 7 Janssen et al.

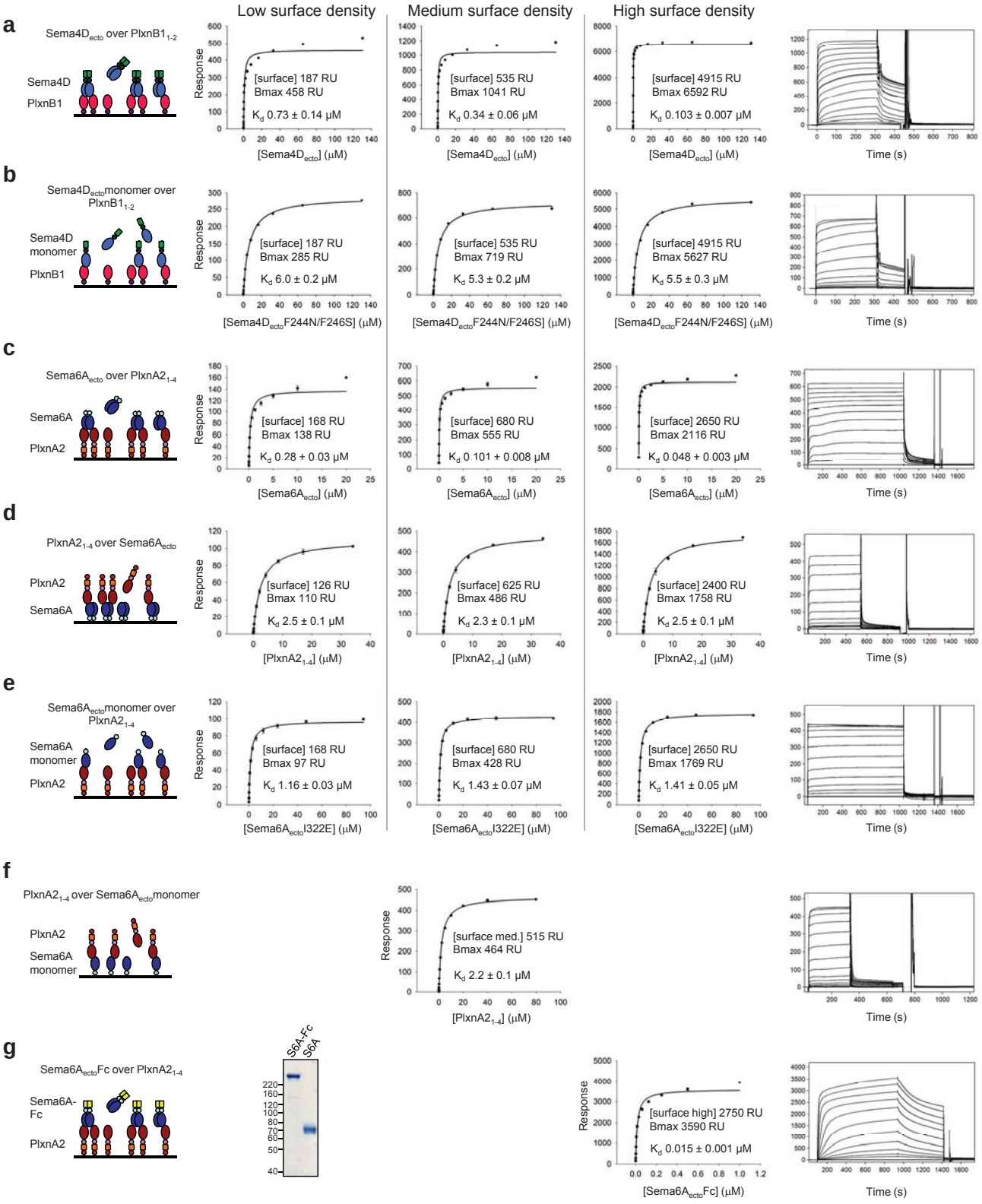

Supplementary Figure 7 Janssen et al.

Supplementary figure 7. Semaphorin binding to plexin is determined by avidity.
SPR equilibrium binding experiments of $PlxnB1_{1-2}$-$Sema4D_{ecto}$ and $PlxnA2_{1-4}$-$Sema6A_{ecto}$ interaction. Models illustrate each SPR experiment (left panels). Three different densities of protein were coupled to the surface to illustrate the effect of bivalent interaction (equilibrium binding plots, middle panels). Representative SPR sensograms of medium surface densities are shown (right panels). **a**, $Sema4D_{ecto}$ binding to $PlxnB1_{1-2}$. The apparent affinities are higher at higher $PlxnB1_{1-2}$ surface densities which is indicative of an avidity effect[22]. The simple 1:1 binding model only fits well where the density of $PlxnB1_{1-2}$ is highest, presumably because most of the interaction is of a bivalent (2:2 and thus 1:1) nature[22]. The fit is worse in the experiments with lower plexin surface densities likely due to mixed bivalent (2:2) and monovalent (1:2) interaction. **b**, The avidity effect is abolished, interactions are monovalent and much weaker when $Sema4D_{ecto}$ is monomerised (see also fig. 3b and supplementary fig. 8a). Interactions fit well to a simple 1:1 binding model, are independent of $PlxnB1_{1-2}$ surface densities and similar to each other (average K_d = 5.6 ± 0.4 μM). **c**, $PlxnA2_{1-4}$-$Sema6A_{ecto}$ interaction has comparable, avidity determined, characteristics as described for the $Sema4D_{ecto}$-$PlxnB1_{1-2}$ interaction in **a**. **d**, The reversed reaction in which $PlxnA2_{1-4}$ monomers bind to $Sema6A_{ecto}$ coupled to the surface is monovalent: interactions are $Sema6A_{ecto}$ surface density independent, fit well to a simple 1:1 binding model and are similar (average K_d = 2.3 ± 0.2 μM, determined from five experiments, two not shown). **e**, Avidity is abolished, interactions are monovalent when $Sema6A_{ecto}$ is monomerised (see also fig. 3a and supplementary fig. 8b) similar to monomeric $Sema4D_{ecto}$F244N/F246S (see **b**) and the average K_d = 1.3 ± 0.2 μM is similar to that determined for the reversed reaction (see **d**). **f**, The affinity of the reversed reaction with monomeric $Sema6A_{ecto}$I322E coupled to the surface is very similar to that of the wild-type interaction as determined in **d**, thus the I322E mutation does not affect the interface with $PlxnA2_{1-4}$. This monovalent interaction is expected to be surface density independent, therefore only one (duplicate) experiment at medium density was performed. **g**, $Sema6A_{ecto}$ is covalently dimerised by a C-terminal Fc tag as shown on non-reducing SDS-PAGE (left panel). The measured apparent affinity is 15.4 ± 1.2 nM at high $PlxnA2_{1-4}$ surface density which is near to those reported for cell-based assays with dimerised semaphorins[2-3].

Supplementary Figure 8 Janssen et al.

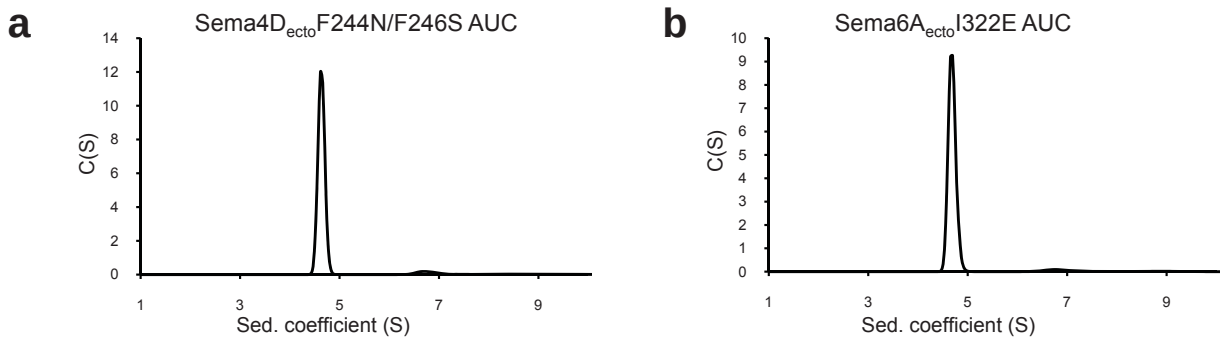

Supplementary figure 8. Sema4D$_{ecto}$F244N/F246S and Sema6A$_{ecto}$I322E are monomers.
Structure based mutations were introduced in the semaphorin homodimerisation interface that we predicted to prevent dimerisation. A glycosylation site was introduced by mutating F244N/F246S in Sema4D$_{ecto}$ and a I322E mutation was introduced in Sema6A$_{ecto}$ (see also fig. 2). Sedimentation velocity analytical ultracentrifugation (AUC) was used to determine that both mutant proteins are induced monomers. **a**, Sedimentation coefficient distribution of Sema4D$_{ecto}$F244N/F246S at a concentration of 2.2 mg/ml. The main peak corresponds to a monomer with a molar mass of about 99 kDa. **b**, Sedimentation coefficient distribution of Sema6A$_{ecto}$I322E at a concentration of 2.2 mg/ml. The main peak corresponds to a monomer with a molar mass of about 83 kDa and the sedimentation coefficient of the Sema6A$_{ecto}$I322E monomer at 4.7 S is different from 7.0 S for the Sema6A$_{ecto}$ dimer (see supplementary fig. 3c).

Supplementary Figure 9 Janssen et al.

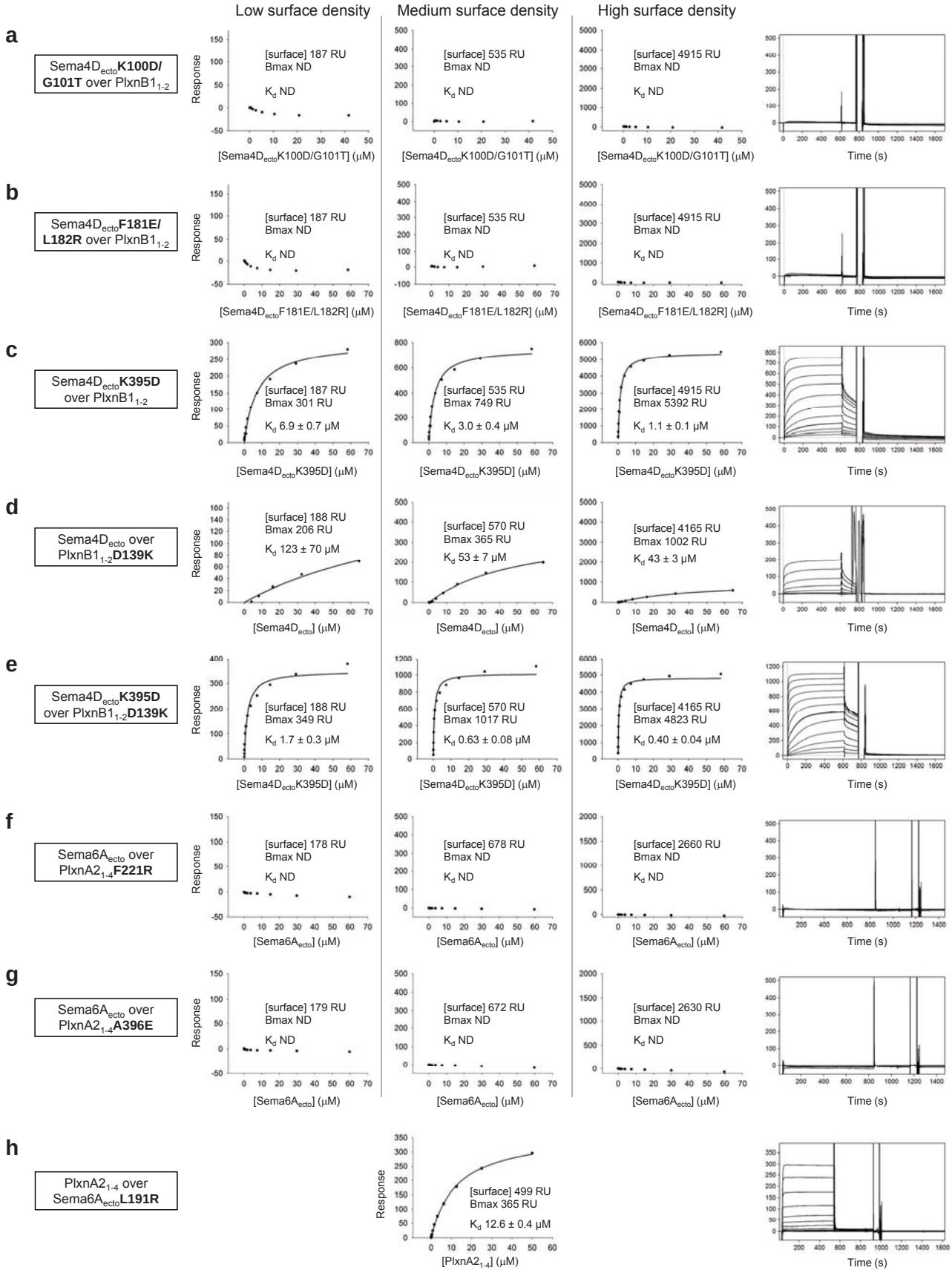

Supplementary Figure 9 Janssen et al.

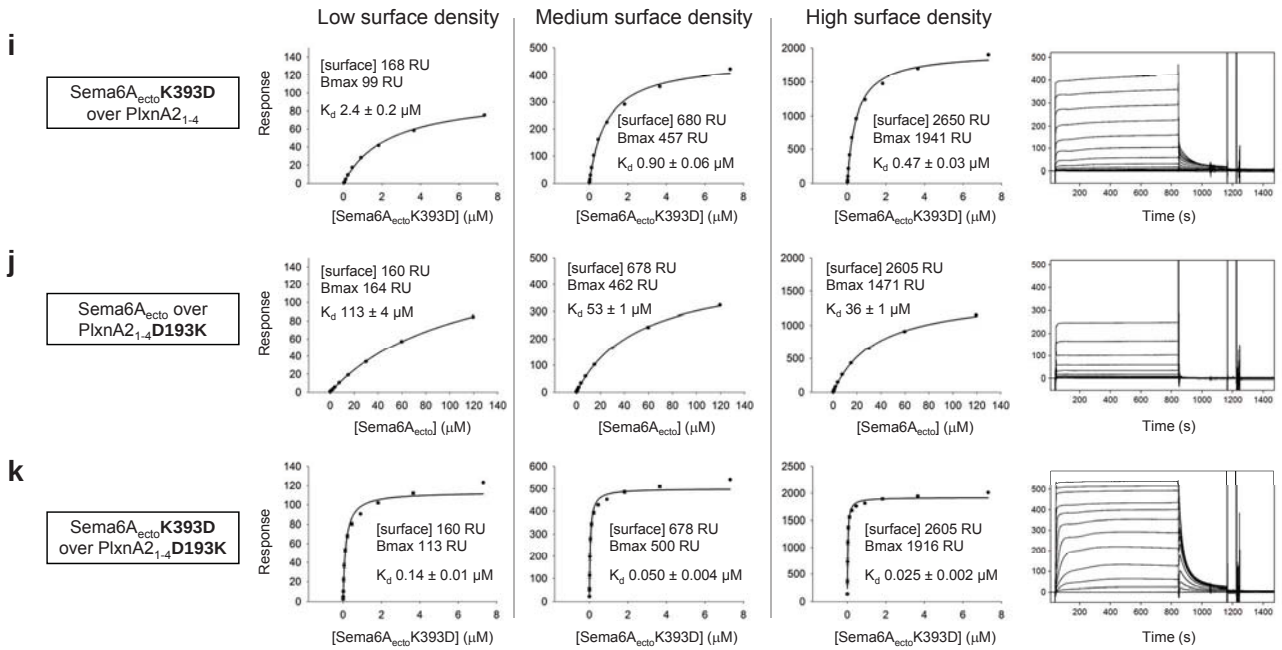

Supplementary figure 9. Semaphorin-plexin interface mutants support the crystal structures. Structure based semaphorin-plexin interface mutants were produced as described in Methods and used in SPR equilibrium binding experiments. Three different densities of protein were coupled to the surface to take into account the effect of bivalent interaction (equilibrium binding plots, middle panels) (see also supplementary fig. 7). Representative SPR sensograms of medium surface densities are shown (right panels). **a** and **b**, The Sema4D$_{ecto}$K100D/G101T and Sema4D$_{ecto}$F181E/L182R mutations completely abolish binding to PlxnB1$_{1-2}$. **c**, Disruption of a conserved salt bridge by the Sema4D$_{ecto}$K395D mutation results in 10 fold weaker binding to PlxnB1$_{1-2}$ as compared to wt Sema4D$_{ecto}$ (see supplementary fig. 7a). **d**, Binding of Sema4D$_{ecto}$ to the PlxnB1$_{1-2}$D139K mutant that disrupts the same salt bridge is over 200 fold weaker as compared to wt PlxnB1$_{1-2}$ (see supplementary fig. 7a). Likely, the apparent affinities in these experiments are even weaker as the predicted Bmax values are lower than expected. **e**, Combining the two mutant proteins (PlxnB1$_{1-2}$D139K and Sema4D$_{ecto}$K395D), thereby reversing the salt bridge, restores the interaction almost completely. This also shows that the mutations do not influence the integrity of the proteins. **f** and **g**, Binding of Sema6A$_{ecto}$ to PlxnA2$_{1-4}$F221R or PlxnA2$_{1-4}$A396E is completely abolished. Interestingly this PlxnA2 A396E mutation has been described previously in mice[11] and fully supports our data. **h**, Binding of PlxnA2$_{1-4}$ to Sema6A$_{ecto}$L191R is 5.5 fold weaker compared to wt Sema6A$_{ecto}$ (see supplementary fig. 7d). **i**, Disruption of the conserved salt bridge by the Sema6A$_{ecto}$K393D mutation results in 9 fold weaker binding to PlxnA2$_{1-4}$ as compared to wt Sema6A$_{ecto}$ (see supplementary fig. 7c). **j**, Binding of Sema6A$_{ecto}$ to the PlxnA2$_{1-4}$D193K mutant that disrupts the same salt bridge is over 500 fold weaker as compared to wt PlxnA2$_{1-4}$ (see supplementary fig. 7c). **k**, By combining the two mutants proteins (PlxnA2$_{1-4}$D193K and Sema6A$_{ecto}$K393D), thereby reversing the salt bridge, binding is fully restored.

Supplementary Figure 10 Janssen et al.

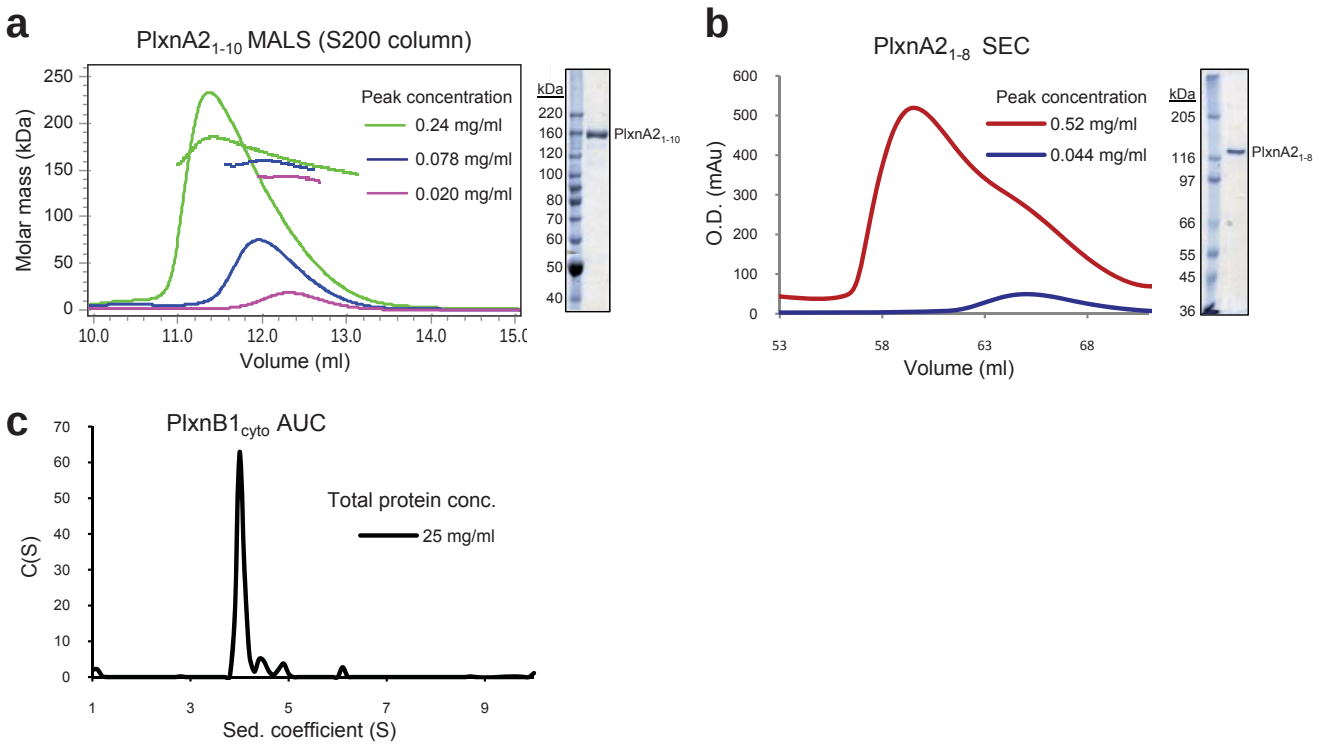

Supplementary figure 10. PlxnA2$_{1-10}$ and PlxnA2$_{1-8}$ both display weak intermolecular interaction, PlxnB1$_{cyto}$ is monomeric.
Multi-angle light scattering (MALS), size-exclusion chromatography (SEC) and sedimentation velocity analytical ultracentrifugation (AUC) revealed that the entire extracellular segment of PlxnA2 (PlxnA2$_{1-10}$) and an eight domain version of PlxnA2 (PlxnA2$_{1-8}$) that lacks the two most membrane proximal IPT domains both have weak intermolecular interaction and that the entire intracellular segment of PlxnB1 (PlxnB1$_{cyto}$) is monomeric in solution. The calculated molar mass for PlxnA2$_{1-10}$ is 153 kDa and 129 kDa for PlxnA2$_{1-8}$ assuming 15% w/w glycosylation. **a**, MALS analysis of PlxnA2$_{1-10}$ showing the molar mass (axis on the left) together with the elution profile (axis not shown) at three different concentrations. The weight average molar mass of PlxnA2$_{1-10}$ determined at a peak concentration of 0.24 mg/ml is 183 ± 2 kDa and indicates that PlxnA2$_{1-10}$ is not exclusively monomeric. At lower concentrations the elution peaks shift to a larger retention volume and the weight average molar masses are slightly reduced and correlate with monomeric PlxnA2$_{1-10}$. This demonstrates that the entire extracellular segment of PlxnA2 has some propensity to undergo weak intermolecular interaction. **b**, Also PlxnA2$_{1-8}$ undergoes a peak-shift upon dilution similar to PlxnA2$_{1-10}$ indicating that it may also have intermolecular interaction. Thus, in contrast to PlxnA2$_{1-4}$ which is monomeric up to concentrations of 2.5 mg/ml (see supplementary figure 3a) PlxnA2 variants that include domains 5-8 can have weak plexin-to-plexin interaction. **c**, Sedimentation coefficient distribution of PlxnB1$_{cyto}$ determined by AUC at a concentration of 25 mg/ml (360 µM). The measured sedimentation coefficient of 4.0 S matches well with the sedimentation coefficient of 4.1 S calculated from the monomeric crystal structure (PDB-ID: 3HM6) using HydroPro (http://leonardo.fcu.um.es/macromol/programs/hydropro/hydropro.htm). Thus PlxnB1$_{cyto}$ is monomeric in solution at a concentration of at least 360 µM and is in agreement with previous results[13].